

Effects of nuclear molecular configurations on the astrophysical S-factor for $^{16}\text{O} + ^{16}\text{O}$

A. Diaz-Torres^a, L.R. Gasques^a and M. Wiescher^b

^a*Department of Nuclear Physics, Research School of Physical Sciences and Engineering, Australian National University, Canberra, ACT 0200, Australia*

^b*Department of Physics and Joint Institute for Nuclear Astrophysics (JINA), University of Notre Dame, Notre Dame, IN 46556, USA*

Abstract

The impact of nuclear molecular configurations on the astrophysical S-factor for $^{16}\text{O} + ^{16}\text{O}$ is investigated within the realistic two-center shell model based on Woods-Saxon potentials. These molecular effects refer to the formation of a neck between the interacting nuclei and the radial dependent collective mass parameter. It is demonstrated that the former is crucial to explain the current experimental data with high accuracy and without any free parameter, whilst in addition the latter predicts a pronounced maximum in the S-factor. In contrast to very recent results by Jiang et al., the S-factor does not decline towards extremely low values as energy decreases.

Key words: Two-center shell model; Woods-Saxon potential; Molecular single-particle states; Nucleus-nucleus potential; Cranking mass parameter; Fusion; S-factor

PACS: 25.60.Pj, 25.70.-z, 21.60.Cs, 26.50.+x

Low-energy fusion reactions involving ^{12}C and ^{16}O are of great astrophysical importance for our understanding of the timescale and the nucleosynthesis during late stellar evolution. Fusion processes like $^{12}\text{C}+^{12}\text{C}$, $^{12}\text{C}+^{16}\text{O}$, and even $^{16}\text{O}+^{16}\text{O}$ characterize the carbon burning phase of massive stars ($M \geq 8M_{\odot}$) with $^{16}\text{O}+^{16}\text{O}$ being the key reaction for the later oxygen burning phase of these stars [1]. The timescale for these burning phases depends on the mass of the star as well as on the reaction rates of the associated fusion processes. The nucleosynthesis during carbon and oxygen burning depends not only on the reaction rate but also on the branching between proton, neutron, or alpha decay channels of the fused compound nucleus [2]. In order to obtain

Email address: alexis.diaz-torres@anu.edu.au (A. Diaz-Torres).

astrophysical reaction rates for different stellar burning scenarios it is crucial to know the fusion cross sections at very low energies. Usually these quantities are extrapolated from theoretical calculations that explain the relatively high-energy fusion data because direct experiments at very low energies are extremely difficult to carry out. The S-factor [1] is an alternative representation of the fusion cross section ($S = \sigma_{fus} E e^{2\pi\eta}$, where η is the Sommerfeld parameter) that facilitates this extrapolation, in particular, for reactions with very light projectiles such as hydrogen or helium because it changes slowly with energy. For heavier nuclei, the S-factor may depend strongly on energy due to the higher Coulomb barriers and angular momenta involved in the fusion process.

The aim of this letter is to show the impact of molecular effects on the astrophysical S-factor for $^{16}\text{O} + ^{16}\text{O}$. The motivation is due to the current discussion in the literature about the behavior of the S-factor excitation function at very low incident energies. Does this function take very small values with decreasing energy? Is there a maximum in the S-factor at energies around 7-8 MeV, as a recent empirical analysis by Jiang et al. [3] suggests? In this work we give a comprehensive answer to these questions by studying the above reaction within the realistic two-center shell model (TCSM) based on spherical Woods-Saxon potentials, as recently reported in Ref. [4]. The $^{16}\text{O} + ^{16}\text{O}$ reaction is a good test case due to its theoretical simplicity (the nuclei are spherical and coupled channels effects are expected to be irrelevant). Furthermore, abundant experimental sub-barrier fusion data [5,6,7,8,9] exist for comparison to the model calculations.

The molecular picture [10] is justified at sub-barrier energies since the radial motion of the nuclei is expected to be adiabatically slow compared to the rearrangement of the mean field of nucleons. We will show that molecular effects related to the formation of a neck between the nuclei and the radial dependent mass parameter are crucial to understand the S-factor excitation function at low energies. Most current theoretical studies use a sudden potential (such as the double-folding potential) and a constant reduced mass (see e.g. Ref. [11]). However, previous works [12,13,14,15] based on either the double oscillator potential or the adiabatic time dependent Hartree-Fock theory have indicated that molecular aspects of the reaction are very important. It is worth mentioning that some light heavy-ion reactions of astrophysical interest have been studied by the Frankfurt group within the concept of nuclear molecules [10] using a restricted TCSM constructed with two harmonic-oscillator potentials.

In the present work, the adiabatic collective potential energy surface $V(R)$ is obtained with Strutinsky's macroscopic-microscopic method, whilst the radial dependent collective mass parameter $M(R)$ is calculated with the cranking mass formula [16]. The rotational moment of inertia of the dinuclear system is defined as the product of the cranking mass and the square of the internuclear

distance. The macroscopic part of the potential results from the finite-ranged liquid drop model with the parameters given in Ref. [17] and the sequence of nuclear shapes generated with the TCSM [4]. The microscopic shell corrections to the potential are calculated with the novel method suggested in Ref. [18]. The TCSM is used to calculate the neutron and proton energy levels E_i as a function of the separation R between the nuclei along with the radial coupling [4] between these levels that appears in the numerator of the cranking mass expression,

$$M(R) = 2\hbar^2 \sum_{i=1}^A \sum_{j>A} \frac{|\langle j | \partial / \partial R | i \rangle|^2}{E_j - E_i}. \quad (1)$$

The parameters of the asymptotic WS potentials including the spin-orbit term reproduce the experimental single-particle energy levels around the Fermi surface of ^{16}O [4], whilst for ^{32}S the parameters of the global WS potential by Soloviev [19] are used, its depth being adjusted to reproduce the experimental neutron and proton separation energies [20]. To describe the amalgamation of two nuclei, the potential parameters have to be interpolated between their values for the separated nuclei and the compound nucleus. The parameters can be correlated by conserving the volume enclosed by certain equipotential surface of the two-center potential for all separations R between the nuclei (see Ref. [4] for further details).

Fig. 1 shows the proton (top) and neutron (bottom) molecular adiabatic levels as a function of the separation between the nuclei. It can be observed that the shell structure of the asymptotic nuclei essentially remains intact (very small polarization of the energy levels) up to the geometrical contact separation ($R_c = 5.85$ fm) that is well inside the s-wave capture barrier (see Fig. 2a - arrow). For radii smaller than R_c (compact shapes) a significant rearrangement of the shell structure of the fusing system occurs. This is reflected in the collective potential energy surface and mass parameter, presented in Fig. 2, by means of the shell correction energy and the virtual excitation of the nucleons (induced by the radial coupling between the single-particle states) to levels above the Fermi surface (open squares), respectively.

Fig. 2a shows the s-wave molecular adiabatic potential (thick solid curve) as a function of the internuclear distance, which is normalized with the experimental Q -value of the reaction ($Q = 16.54$ MeV). The sequence of nuclear shapes related to this potential [4] is also presented. For comparison we show the Krappe-Nix-Sierk (KNS) potential [22] (thin solid curve) and the empirical Broglia-Winther (BW) potential [23] (dotted curve). Effects of neck between the interacting nuclei, before they reach the geometrical contact separation, are not incorporated into the KNS potential. The concept of nuclear shapes is not embedded in the BW potential which tends to be similar to the KNS

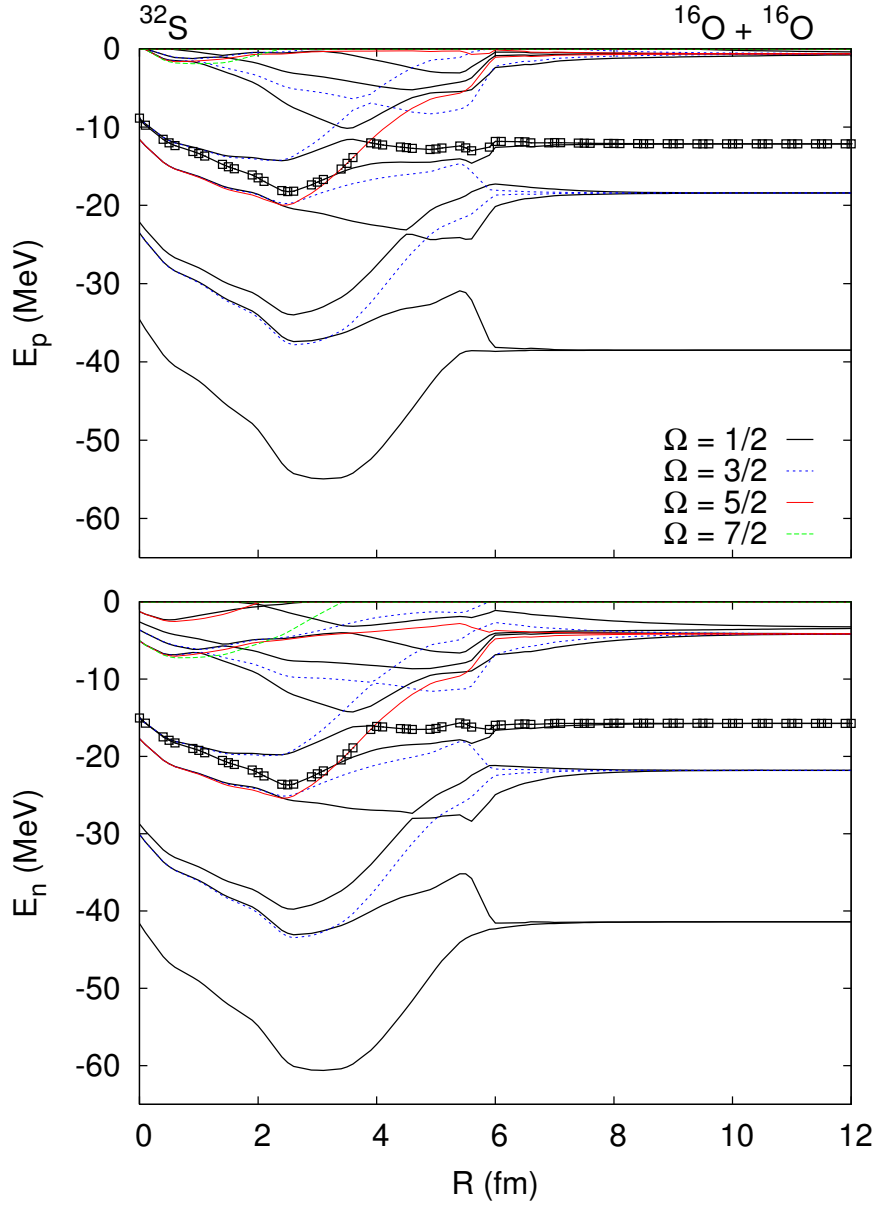


Fig. 1. (Color online) Molecular adiabatic single-particle levels as a function of the separation between the nuclei: protons (top) and neutrons (bottom). Different types of curve refer to states with different projection of the nucleon total angular momentum along the internuclear axis. The open squares denote the Fermi surface. See text for further details.

potential. Comparing the KNS potential to the molecular adiabatic potential we note that the neck formation substantially decreases the potential energy after passing the barrier radius ($R_b = 8.4$ fm). It will be shown that the inclusion of neck effects is crucial to successfully explain the available S-factor data [5,6,7,8,9] for the studied reaction.

Fig. 2b shows the radial dependent cranking mass (thick solid curve), whilst

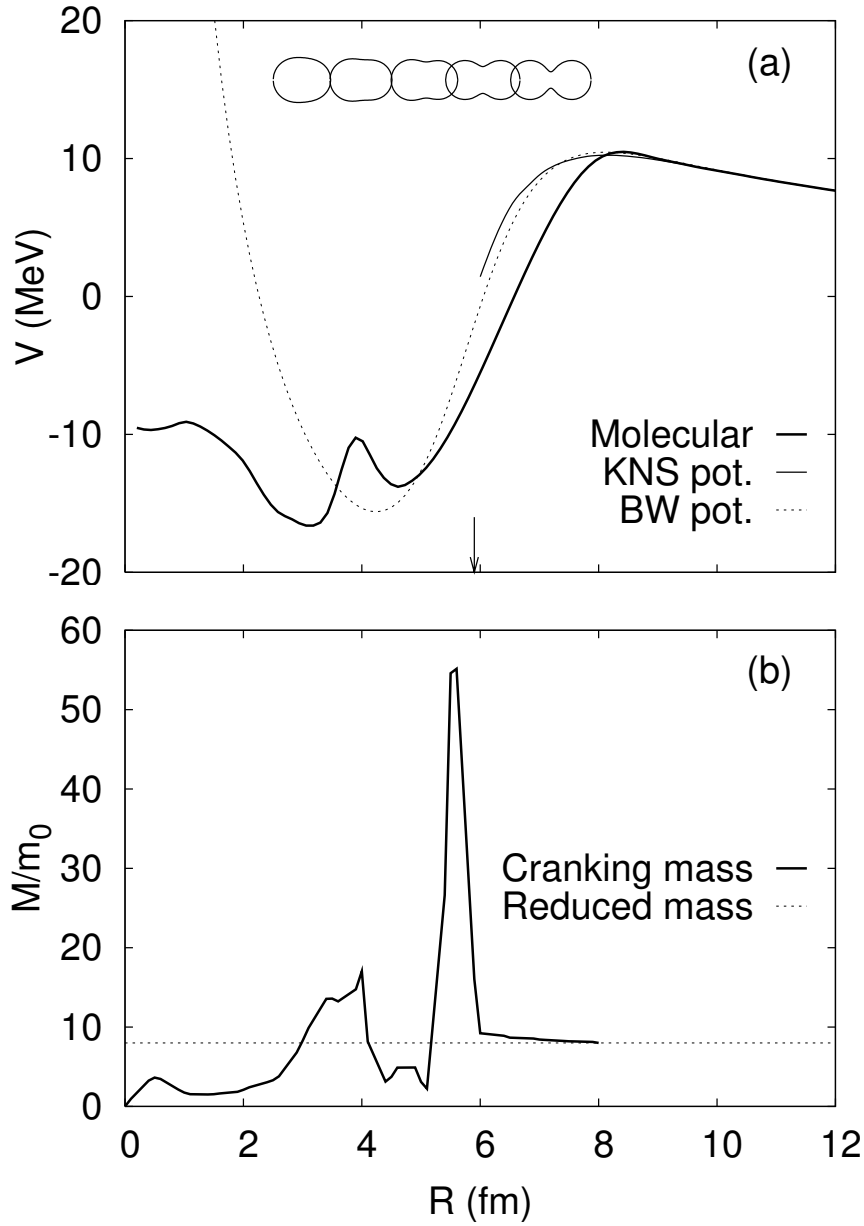


Fig. 2. (a) The s-wave collective potential energy as a function of the separation between the nuclei for $^{16}\text{O} + ^{16}\text{O}$. The arrow indicates the geometrical contact separation. (b) The radial dependent collective mass parameter (in units of nucleon mass m_0). See text for further details.

the asymptotic reduced mass is indicated by the dotted line. Just passing the barrier radius, when the neck between the nuclei starts to develop, the cranking mass slightly increases compared to the reduced mass and pronounced peaks appear inside the geometrical contact separation. For the studied reaction, these peaks are mainly caused by the strong change of the single-particle wave functions during the rearrangement of the shell structure of the asymptotic nuclei into the shell structure of the compound system [large values of the

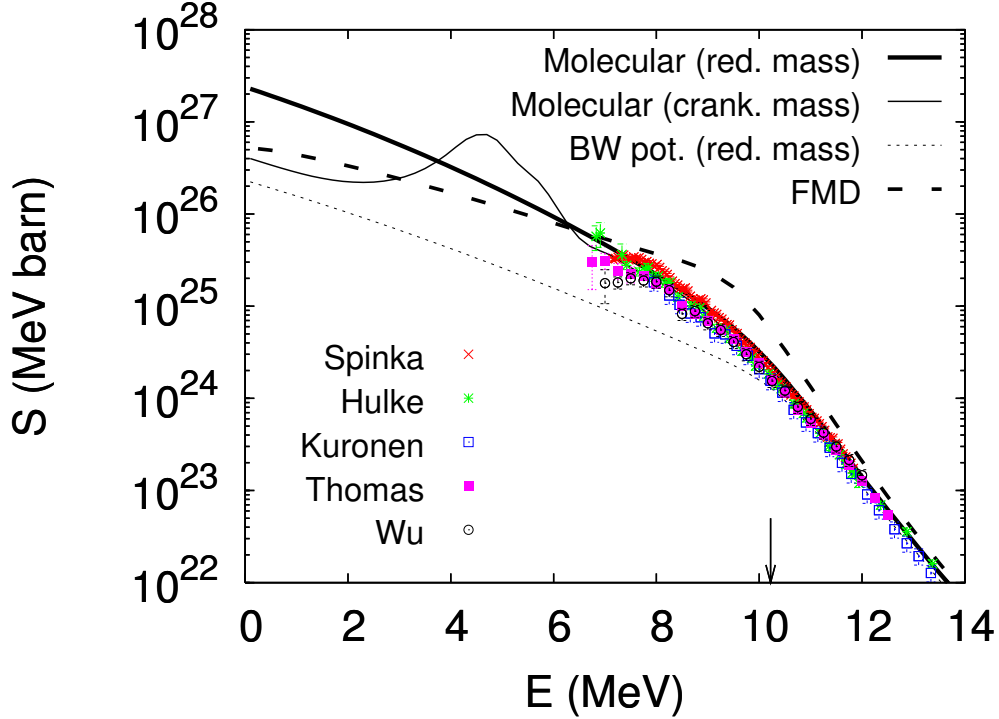


Fig. 3. (Color online) The S-factor as a function of the center-of-mass energy for $^{16}\text{O} + ^{16}\text{O}$. The curves are theoretical calculations, whilst the symbols refer to experimental data. The arrow indicates the Coulomb barrier of the molecular potential of Fig 2a. See text for further details.

radial coupling in the numerator of the cranking mass formula (1)]. In general, the peaks could also be due to avoided crossings [4] between the adiabatic molecular single-particle states (see Fig. 1), which can make the denominator of the cranking mass expression (1) very small.

Having the adiabatic potential and the adiabatic mass parameter, the radial Schrödinger equation is exactly solved with the modified Numerov method [21] and the incoming wave boundary condition imposed inside the capture barrier. The fusion cross section σ_{fus} is calculated taken into account the identity of the interacting nuclei and the parity of the wave function for the relative motion (only even partial waves L are included here), i.e., $\sigma_{fus} = \pi\hbar^2/(2\mu E) \sum_L (2L+1)(1+\delta_{1,2})P_L$, where μ is the asymptotic reduced mass, E is the incident energy in the total center-of-mass reference frame and P_L is the partial tunneling probability.

Fig. 3 shows the S-factor as a function of the incident energy in the center-of-mass reference frame. For a better presentation, the experimental data of each set [5,6,7,8,9] are binned into $\Delta E = 0.5$ MeV energy intervals. In this figure the following features can be observed:

- (i) the molecular adiabatic potential of Fig. 2a correctly (thick and thin solid

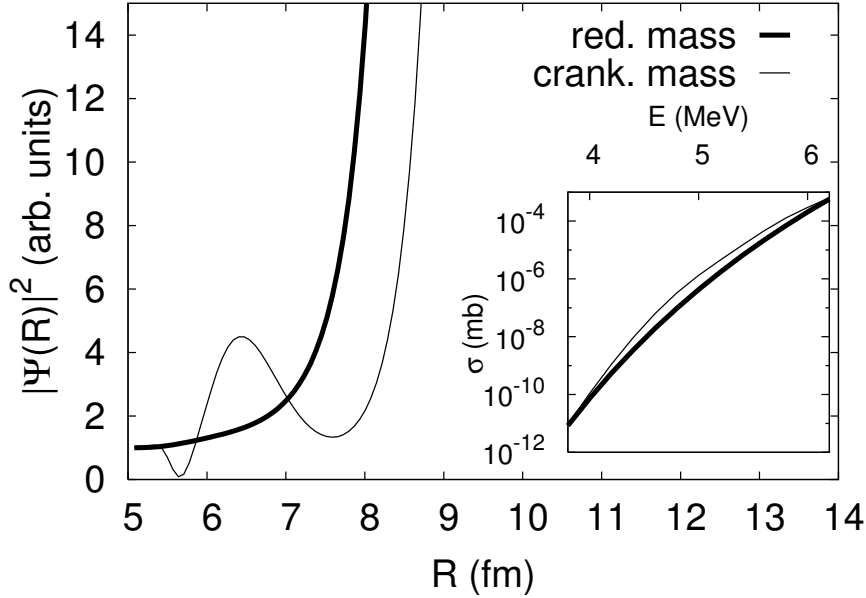


Fig. 4. Probability distribution of the collective radial wave function for the s-wave calculated with the reduced mass and the cranking mass at an incident energy of 4.5 MeV. The strong peak of the cranking mass in Fig. 2b makes it most probable for the molecular configuration (trapped inside the barrier) to be localized just before the geometrical contact separation (6-7 fm), which increases the fusion cross section (small figure inserted) and causes the local maximum of the S-factor in Fig. 3. See text for further details.

curves) explains the measured data, in contrast to either the results obtained with the BW potential (dotted curve) or the very recent calculations by Neff et al. [24] within the Fermionic Molecular Dynamics (FMD) approach (dashed curve). Since the width of the barrier decreases for the molecular adiabatic potential of Fig. 2a, it produces larger fusion cross sections than those arising from the shallower KNS and BW potentials.

- (ii) the use of the cranking mass parameter of Fig. 2b notably affects the low energy S-factor, which is revealed by the comparison between the thick and thin solid curves. It starts reducing the S-factor around 7-8 MeV energy region and produces a local maximum around 4.5 MeV. At the lowest incident energies (below 4 MeV) the S-factor is suppressed by a factor of five compared to that arising from a constant reduced mass. The peak in the S-factor is due to an increase of the fusion cross section (see Fig. 4), which is caused by the resonant behavior of the collective radial wave function increasing the fusion transmission coefficient.

Since we have solved a single-channel Schrödinger equation (elastic channel) with the incoming wave boundary condition, which is equivalent to a very strong absorption inside the barrier, we do not see any molecular resonances for the lowest partial waves leading to fusion. However, few of them may exist for the grazing waves which should be reflected in direct reaction channels

[25]. At incident energies higher than those studied in the paper (i.e., $E \gtrsim 20$ MeV), we expect that strong inelastic channels will be open, and the molecular resonances could impact not only on the elastic, inelastic and transfer excitation functions but also on the fusion excitation function. Here a molecular Coupled Reaction Channels (CRC) description [10] will be required.

In summary, the adiabatic molecular potential appears to be crucial to explain, with high accuracy and without any free parameter, the existing experimental data of the S-factor for the reaction $^{16}\text{O} + ^{16}\text{O}$. More interesting, the radial cranking mass impacts significantly on the S-factor excitation function at very low energies, where no experimental data are available. Clearly, it causes a pronounced maximum around 4.5 MeV in the S-factor excitation function. To verify this effect new experiments are very desirable. In contrast to the results reported in Ref. [3], the S-factor does not decline towards extremely low values with decreasing energy. In fact, below 4 MeV, the S-factor is only suppressed by a factor of five with respect to the calculation with the constant reduced mass. The molecular picture discussed in this work could also be applied to other light systems of great astrophysical interest that involves deformed nuclei such as $^{12}\text{C} + ^{12}\text{C}$ and $^{12}\text{C} + ^{16}\text{O}$, provided a general TCSM for arbitrarily-orientated deformed nuclei is employed. This work is in progress, and the results will appear in a forthcoming publication.

Acknowledgement

This work was supported by the Joint Institute for Nuclear Astrophysics (JINA) through grant NSF PHY 0216783, and by the ARC Discovery grant DP0557065.

References

- [1] C.E. Rolfs and W.S. Rodney, *Cauldrons in the Cosmos* (The University of Chicago Press, Chicago, 1988).
- [2] M. Wiescher, R.E. Azuma, L.R. Gasques, J. Görres, M. Pignatari, E. Simpson, *Mem. S. A. It.* **77**(2006) 910.
- [3] C.L. Jiang, K.E. Rehm, B.B. Back and R.V.F. Janssens, *Phys. Rev. C* **75**(2007) 015803.
- [4] A. Diaz-Torres and W. Scheid, *Nucl. Phys. A* **757**(2005) 373.
- [5] H. Spinka and W. Winkler, *Astrophys. J.* **174**(1972) 455.
- [6] G. Hulke, C. Rolfs and H.P. Trautvetter, *Z. Phys. A* **297**(1980) 161.
- [7] A. Kuronen, J. Keinonen and P. Tikkanen, *Phys. Rev. C* **35**(1987) 591.

- [8] J. Thomas, Y.T. Chen, S. Hinds, D. Meredith and M. Olson, *Phys. Rev. C* **33**(1986) 1679.
- [9] S.C. Wu and C.A. Barnes, *Nucl. Phys. A* **422**(1984) 373.
- [10] W. Greiner, J.Y. Park and W. Scheid, *Nuclear Molecules*, World Scientific, Singapore, 1994.
- [11] D.G. Yakovlev, L.R. Gasques, A.V. Afanasjev, M. Beard and M. Wiescher, *Phys. Rev. C* **74**(2006) 035803.
- [12] H. Flocard, P.H. Heenen and D. Vautherin, *Nucl. Phys. A* **339**(1980) 336.
- [13] P.H. Heenen, *Phys. Lett. B* **99**(1981) 298.
- [14] N. Urbano, K. Goeke and P.-G. Reinhard, *Nucl. Phys. A* **370**(1981) 329.
- [15] P.-G. Reinhard, J. Friedrich, K. Goeke, F. Grümmer and D.H.E. Gross, *Phys. Rev. C* **30**(1984) 878.
- [16] D.R. Inglis, *Phys. Rev.* **103**(1956) 1786.
- [17] P. Möller and J.R. Nix, *Atomic Data and Nuclear Data Tables* **26**(1981) 165.
- [18] A. Diaz-Torres, *Phys. Lett. B* **594**(2004) 69.
- [19] V.G. Soloviev, *Theory of Complex Nuclei* (Pergamon Press, Oxford, 1976) p. 21.
- [20] G. Audi and A.H. Wapstra, *Nucl. Phys. A* **565**(1993) 1.
- [21] M.A. Melkanoff, T. Sawada and J. Raynal, *Meth. Comput. Phys.* **6**(1966) 1.
- [22] H.J. Krappe, J.R. Nix and A.J. Sierk, *Phys. Rev. C* **20**(1979) 992.
- [23] W. Reisdorf, *J. Phys. G* **20**(1994) 1297.
- [24] T. Neff, H. Feldmeier and K. Langanke, arXiv: nucl-th/ **0703030**.
- [25] G. Gaul and W. Bickel, *Phys. Rev. C* **34**(1986) 326.